ACES Asian Chemical Editorial Society

doi.org/10.1002/asia.202300950

CHEMISTRY AN ASIAN JOURNAL Research Article

www.chemasianj.org

At the limits of bisphosphonio-substituted stannylenes

Sina Nasemann,[a] Roman Franz,[a] Denis Kargin,[a] Clemens Bruhn,[a] Zsolt Kelemen,[b] Torsten Gutmann,[c] and Rudolf Pietschnig*[a]

Donor stabilization of Sn(II) and Pb(II) halides with 1,1′-ferrocenylene bridged bisphosphanes has been explored for $Fe(C_5H_4P(C_6H_5)_2)_2$ (dppf), and $Fe(C_5H_4PH(C_4H_9))_2$. These bisphosphanes are reacted with $SnBr_2$ and $PbCl_2$ with and without additional Lewis acid ($AlCl_3$) forming acyclic and cyclic donor adducts from which the latter represent bisphosphoniotetrylenes. Since dynamic exchange in solution is observed, characterization includes solution and solid-state NMR in addition to SC-XRD, amended by DFT calculations.

Introduction

Heavier tetrylenes like other hetero-carbenes experience pronounced stabilization from adjacent π-donating substituents limiting the acceptor properties of the low-valent atom.[1] A landmark in this respect was the first example of an isolable all carbon substituted silylene lacking such π-donor substituents.[2] The strategy of replacing nitrogen with phosphorus in *N*-heterocyclic tetrylenes and hetero-carbenes has also furnished remarkable results demonstrating the higher electrophilicity of the low-valent atom by formation of mutual donor acceptor adducts via 1,2-[3] or 1,1-dimerization[4] in addition to very few monomeric examples.[5] Owing to the predominant s-character of the lone-pair in phosphanyl groups the π-donating properties are already quite limited, apart from special cases.[6] Quaternization of the phosphorus atoms is expected to suspend mesomeric stabilization completely and the corresponding bisphosphonio tetrylenes likewise may be described as bisphosphane complexes of the corresponding tetrel dications (Figure 1). Previous work on Sn(II) coordination indicates a strong dependence on the counter anion,[7] ligand hapticity[8] and even partial bond activation at the ligand.[9] Interestingly, dative N–Sn-coordination was found to be preferred over isomeric P–Sn donation.[10] Here we employ 1,1′-ferrocenylene bridged bisphosphanes aiming at the preparation of the corresponding cationic bisphosphonio stannylenes.

Results and Discussion

As a starting point we explored the coordination of Sn(II) to bis(diphenylphosphanyl)ferrocene (dppf) a commercially available bisphosphane with well documented donor-properties. The dppf was reacted with 2 eq. of $SnBr_2$ since in related cases the second equivalent acted as halide abstracting Lewis acid (Scheme 1).

NMR studies in solution (CH_2Cl_2) indicate a dynamic equilibrium with significant line broadening. While the ^{119}Sn resonance at ca. −13 ppm ($\nu_{1/2}$ = 278 Hz) is significantly deshielded with respect to the starting material $SnBr_2$, the ^{31}P, ^{1}H, and ^{13}C NMR signals of the dppf remain almost unchanged (ESI, Figure S4). Evaporation of the solvent leads to an orange crystalline product **2**. SC-XRD on suitable crystals of **2** revealed its molecular structure in which each phosphorus atom coordinates a $SnBr_2$ unit in an acyclic fashion (Figure 2).

Since the hypothesis that $SnBr_2$ would also act to abstract halide could not be confirmed, we considered a more pronounced Lewis acid for this purpose. To this end we reacted dppf with $SnBr_2$ and $AlCl_3$ simultaneously (Scheme 2). In

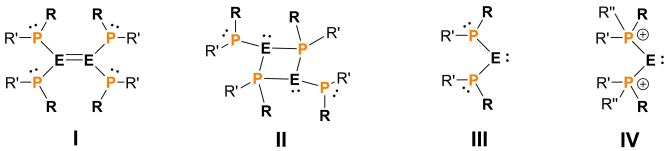

Figure 1. Sketch of heavier bisphosphanyltetrylenes in 1,1-dimeric **(I)**, 1,2-dimeric **(II)**, monomeric **(III)** and quaternized **(IV)** form (E = Sn; R, R′ = organic/organometallic substituent).

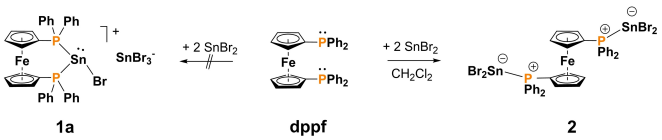

Scheme 1. Coordination of Sn(II) with dppf.

[a] S. Nasemann, Dr. R. Franz, Dr. D. Kargin, Dr. C. Bruhn, Prof. Dr. R. Pietschnig
Department of Chemistry
University of Kassel
Heinrich-Plett-Str. 40, 34132 Kassel, Germany
E-mail: pietschnig@uni-kassel.de

[b] Dr. Z. Kelemen
Department of Inorganic and Analytical Chemistry
Budapest University of Technology and Economics
Műegyetem Rkp. 3 H-1111 Budapest, Hungary

[c] Prof. Dr. T. Gutmann
Eduard Zintl Institute for Inorganic and Physical Chemistry
Technical University of Darmstadt
Peter-Grünberg-Straße 8, 64287 Darmstadt, Germany

Supporting information for this article is available on the WWW under https://doi.org/10.1002/asia.202300950

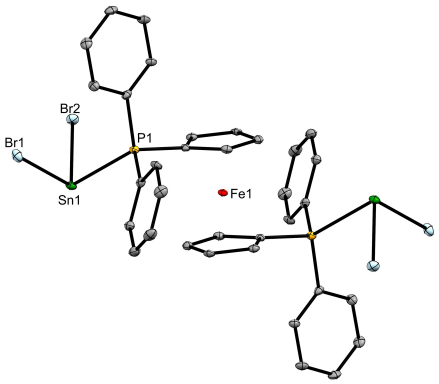

Figure 2. Molecular structure of **2**. Ellipsoids are drawn at 30% probability level and all hydrogen atoms are omitted for clarity. Selected bond lengths: Sn1-P1 2.7284(10) Å; Sn1-Br1 2.5906(5) Å; Sn1-Br2 2.5849(5) Å.

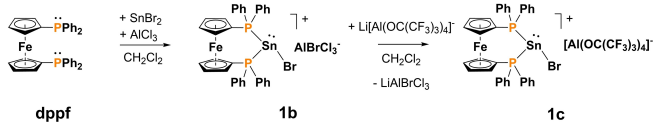

Scheme 2. Coordination of Sn(II) with dppf in presence of an additional Lewis acid followed by anion exchange.

solution (CH_2Cl_2) the ^{31}P as well as the ^{119}Sn resonances were both deshielded and broadened ($\delta(^{31}P)$: −2.1 ppm, $\nu_{1/2}$ = 120 Hz; $\delta(^{119}Sn)$: −24.4 ppm, $\nu_{1/2}$ = 70 Hz). The ^{27}Al-NMR data were further complicated by halide scrambling indicating the presence of tetrachloroaluminate (δ = 103.8 ppm, $\nu_{1/2}$ = 52 Hz), bromotrichloroaluminate (δ = 100.0 ppm, $\nu_{1/2}$ = 78 Hz), dibromodichloroaluminate (δ = 95.0 ppm, $\nu_{1/2}$ = 86 Hz), and tribromochloroaluminate (δ = 88.6 ppm) in reasonable agreement with literature data.[11]

To avoid dynamic halide exchange, the anion of compound **1b** was exchanged by reaction with $Li[Al(OC(CF_3)_3)_4]$ (Scheme 2). The observation of narrow resonances with resolved P–Sn couplings visible in the ^{31}P- and ^{119}Sn-NMR spectra confirms the absence of dynamic exchange as intended. The ^{31}P-NMR spectra show a narrow singlet at 3.9 ppm ($\nu_{1/2}$ = 4 Hz) with $^1J_{PSn}$ = 1751 Hz (^{119}Sn isotopomer) and $^1J_{PSn}$ = 1670 Hz (^{117}Sn isotopomer), shifted 6 ppm downfield compared to **1b**. The ratio between the central resonance and the satellites for the signal at 3.9 ppm with a value of 85:15 is indicative for a single tin atom bridging the two phosphorus atoms. In the corresponding ^{119}Sn-NMR spectrum a triplet at 0.1 ppm corroborates the bridging situation with the matching coupling constant $^1J_{PSn}$ = 1751 Hz and is in agreement with $^1J_{PSn}$ literature values for the SnCl-fragment chelated by $[(Ph_2PCH_2)_2BPh_2]$ ($^1J_{PSn}$ = 1794 Hz).[9]

Although the identity of **1c** is evident from the complete set of heteronuclear NMR spectra, traces of the analogous aluminum bridged diphospha-[3]ferrocenophane $[Fe(CpPPh_2)_2AlCl_2][Al(OC(CF_3)_3)_4]$, could not be removed (cf. ESI for details).

Moving to the heavier tetrel, we explored the reaction of dppf with $PbCl_2$. Again dppf was exposed to two equivalents of lead(II) chloride in dichloromethane (CH_2Cl_2). Even after several days of stirring at room temperature no reaction with $PbCl_2$ was observed, which did not change by the addition of equimolar amounts of aluminium(III) chloride. Although no reaction involving lead occurred, NMR spectroscopy revealed that rather aluminium coordinates to dppf. Therefore, the direct reaction between dppf and $AlCl_3$ in the absence of $PbCl_2$ was explored (Scheme 3).

In CD_2Cl_2 solution the ^{31}P-chemical shift of the dppf resonance at −17.7 ppm is hardly affected by the addition of aluminium(III) chloride whereas the signal broadening increases with the amount of *Lewis*-acid (**3**: −17.8 ppm, $\nu_{1/2}$ = 28 Hz and **4**: −18.1 ppm, $\nu_{1/2}$ = 158 Hz), in agreement with previously reported complexes of dppm and dppe with aluminium(III) chloride.[12]

Further confirmation of adducts **3** and **4** is obtained in the ^1H- and even more pronounced in the ^{13}C-NMR spectra. The multiplets of the Cp-resonances in the proton NMR spectra are deshielded upon $AlCl_3$ coordination by ca. 0.4 ppm as compared to dppf. Owing to fast exchange on the NMR time scale, the signals of the non-coordinated and the coordinated units in **3** are observed as averaged signals in between those in **4** and dppf. In the ^{13}C-NMR spectra the carbon atoms adjacent to phosphorus are most affected by the adduct formation. Both types of nuclei experience significant shielding compared with dppf. In **4** the signal for phenyl *ipso*-C at 126 ppm is shifted to higher field by more than 13 ppm and the one for the Cp_q at 67 ppm is shifted upfield by 10 ppm. Additionally, the related $^1J_{PC}$ coupling constants increase significanly by 43 Hz to 54 Hz (Ph_q) and 50 Hz to 58 Hz (Cp_q). Comparable trends of the NMR parameters have already been observed for dppe and its aluminium chloride adducts.[12] The ^{27}Al-NMR spectrum of **3** shows a broad signal at 109.9 ppm ($\nu_{1/2}$ = 750 Hz). A visually identical shift is observed for **4** (109.8 ppm, $\nu_{1/2}$ = 740 Hz). These values are in agreement with literature known values for the structurally related dppe mono-$AlCl_3$ adduct ($\delta(^{27}Al)$: 109.3 ppm ($\nu_{1/2}$ = 600 Hz)) and the bis-$AlCl_3$ adduct ($\delta(^{27}Al)$: 108.8 ppm ($\nu_{1/2}$ = 600 Hz)).[12] Coupling between phosphorus and aluminium was neither observed in ^{27}Al- nor in ^{31}P-NMR spectra. However, *Reid et al.* were able to resolve the $^1J_{PAl}$ coupling constant of 275 Hz for the similar system $[AlCl_3(PMe_3)]$ but only at low temperature.[13] Elemental analysis of the reaction products in presence and absence of $PbCl_2$ confirms that in both cases the aluminium-monoadduct **3** is formed. ssNMR measurements of **3** (ESI, Figures S6-S8) support the formation of a mono-phosphanyl-coordinated aluminium adduct showing two signals in the ^{31}P CP MAS spectrum. The resonance at −17.8 ppm is in agreement with the ^{31}P-NMR chemical shift of **3** in solution and is assigned to the phosphorus atom attached to the aluminium, whereas the sharp signal at −14.7 ppm is assigned to the free

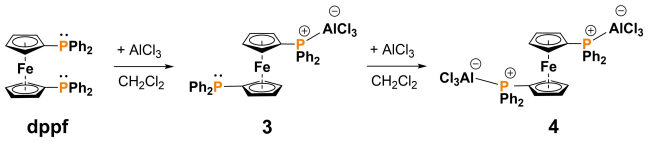

Scheme 3. Adducts of dppf with $AlCl_3$.

phosphanyl unit of **3** in agreement with the ^{31}P CP MAS spectrum of the neat dppf ligand (ESI, Figure S1). Furthermore, the *J*-resolved ^{31}P-ssNMR spectrum (ESI, Figure S7) shows no resolvable coupling between both phosphorus nuclei, indicating the formation of **3**, while bridging of both phosphanyl units by a single aluminium nucleus can be excluded. The corresponding ^{27}Al MAS spectrum shows a dominant resonance at 104 ppm for **3** (ESI, Figure S8) consistent with the chemical shift in solution (*v.s.*). Similarly, neither in the ^{31}P CP MAS nor the ^{27}Al MAS spectra a P–Al coupling can be resolved, just as in solution.

Structural evidence for formation of adduct **4** is provided by SC-XRD. Adduct **4** crystallizes in the triclinic space group $P\bar{1}$. The phosphorus atoms are found in *anti* conformation (Figure 3). The bond lengths of P1-Al1 2.4211(18) Å and P2-Al2 2.4037(16) Å are comparable to those of similar, tertiary phosphane complexes of tetracoordinate aluminum such as $AlX_3(PR_3)$ (X = Cl, Br and R = Me, $SiMe_3$) with P–Al 2.391(6) Å to 2.4059(14) Å.[13–14] The Al–Cl bond lengths cover distances from 2.107(2) to 2.127(2) Å and are in agreement with corresponding bonds in e.g. $AlCl_3P(SiMe_3)_3$ (2.112–2.125 Å).[13]

Since dppf was unfavorable for bridging the two phosphanyl groups with Sn(II) and Pb(II) in an intermolecular fashion we switched to the sterically less challenged bisphosphane **5** which has been successfully employed in preparing neutral bisphosphanyltetrylenes in the past.[3a,b] In addition, bisphosphane **5** shows superior σ-donor properties than dppf as indicated by the $^{1}J_{PSe}$ coupling constants of the corresponding selenides *i.e.*, 761 Hz (**dppf•Se$_2$**, toluene-d_8) vs. 729/731 Hz (*rac/meso*-**5•Se$_2$**, C_6D_6).[15] Reacting bisphosphane **5** with $SnBr_2$ in a 1:2 ratio in dichloromethane results in the formation of PSn^{II}P [3]ferrocenophane **6a** as intended. When DMSO or coordinating solvents like tetrahydrofuran (THF) or dimethylol ethylene urea (DMEU) are added, a back-reaction takes place leading to the starting compound **5** together with a donor solvent-$SnBr_2$ adduct. Compound **6a** shows two broad ^{31}P-NMR resonances at −5.0 ppm ($\nu_{1/2}$ = 170 Hz, 90%) and 6.7 ppm ($\nu_{1/2}$ = 190 Hz, 10%). Isomers of compound **6a** could arise from *rac* and *meso* diastereomers or *cis* and *trans* isomers of *meso*-**6a** with respect to the orientation of the bromine atom to the substituents at the phosphorus atoms. In structurally related P–X–P bridged [3]ferrocenophanes (X = B, Si, P), predominantly the optically inactive *meso*-form was formed except for P–B–P bridged [3]ferrocenophanes.[16] Our DFT calculations indicate a moderate preference for the *cis* isomer which is only 0.5 kcal/mol more stable than its *trans* isomer (wB97x-D/def2-TZVP). The low energy difference is consistent with the observation of both isomers. Since the occurrence of *rac* and *meso* isomers would entail additional isomers, which are not observed, we assign the major isomer of **6a** to its *cis* form and the minor isomer to its *trans* form.

Accordingly, the hydrogen atoms at phosphorus show doublets at 6.90 ppm ($^{1}J_{PH}$ = 374.1 Hz, *cis* isomer) and 6.04 ppm ($^{1}J_{PH}$ = 364.4 Hz *trans* isomer) in the ^{1}H-NMR-spectra. These resonances are strongly deshielded compared with the starting material, **5** ($\delta(^{1}H)$ = 3.84 and 3.81 ppm, $^{1}J_{PH}$ = 210 and 209 Hz, in CD_2Cl_2), in line with the phosphonium character of the respective protons. Despite **6a** containing two chemically inequivalent tin atoms, only a single broad signal at 130 ppm ($\nu_{1/2}$ = 1370 Hz) is found in the ^{119}Sn-NMR-spectrum without resolved $^{117/119}$Sn-^{31}P coupling consistent with the absence of tin satellites in the ^{31}P-NMR spectra. Structurally related literature known compounds show $^{1}J_{PSn}$ coupling constants in the range of 720–1200 Hz.[3b] A conceivable reason for not observing satellites is dynamic behavior in solution, which is known to cause broader signals in the related NMR spectra.[17] To circumvent the dynamic behavior in solution, solid-state NMR measurements of compound **6a** were performed. ^{31}P CP MAS NMR spectra of **6a** (ESI, Figure S11) show two signals of similar intensity with tin satellites at −7.0 ppm ($^{1}J_{PSn}$ = 1215 Hz) and −17.5 ppm ($^{1}J_{PSn}$ = 1580 Hz). The corresponding ^{119}Sn static spectrum (ESI, Figure S12) shows two broad signals with isotropic shifts at −4.5 ppm and −199 ppm. These signals are assigned to the $[SnBr_3]^-$ anion and to the bridging Sn-atom of the ferrocenophane backbone, respectively. Since the ^{119}Sn-^{31}P couplings were unresolved in the ^{119}Sn static spectrum, unambiguous signal assignment is difficult.

The formation of adduct **6a** was further corroborated by SC-XRD (Figure 4). Compound **6a** crystallizes in the *meso cis* form as yellow plates in the monoclinic space group $P2_1/c$. The

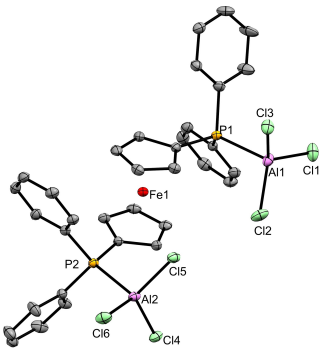

Figure 3. Molecular structure of **4**. Ellipsoids are drawn at 30% probability level and all hydrogen atoms are omitted for clarity. Selected bond lengths: P1-Al1 2.4211(18) Å, P2-Al2 2.4037(16) Å.

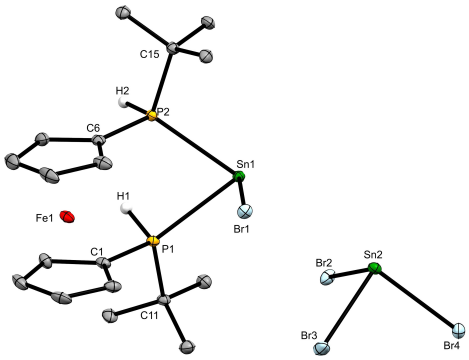

Figure 4. Molecular structure of adduct **6a** with ellipsoids drawn at 30% probability level and hydrogen atoms, except for PH, omitted for clarity. Selected bond lengths and angles: Sn1-P1 2.7404(9) Å; Sn1-P2 2.7394(8) Å; Sn1-Br1 2.6155(4) Å; P1-H1 1.29(3) Å; P2-H2 1.32(4) Å; Br1-Sn1-P1 95.56(2)°; Br1-Sn1-P2 87.02(2)°, P1-Sn1-P2 77.79(3)°.

P–Sn-P bridge causes a slight inclination of the Cp rings towards the bridge (tilt angle α = 3.8(2)°). This value indicates no ring tension in the molecule, consistent with α angles found in the literature for P–X–P [3]ferrocenophanes (X = Si, P).[3a,18] The P–Sn-P angle of 77.79(3)° in **6a** is close to the values observed for P–X-P angles in tetrylene adducts with [3]ferrocenophane scaffold (X = Si, Sn, Pb).[3a,b] The angular sum at Sn1 (260(2)°) indicates a trigonal pyramidal geometry with a stereochemically active non-bonding electron pair (compare **5-Sn** *trans:* 280°, *cis*: 273°).[19]

The P–H bond length increases upon coordination to the SnBr fragment, showing bond lengths of P1-H1 1.29(3) Å and P2-H2 1.32(4) Å compared to the P–H bond lengths of the starting material (P–H 0.76(4) Å).[20] Symmetric contacts are found between tin and both phosphorus atoms with bond lengths of Sn1-P1 2.7404(9) Å and Sn1-P2 2.7394(8) Å. Compared to the structurally related dimeric bisphosphanylstannylenes (P–Sn bond lengths between 2.588(6) and 2.665(5) Å),[3b] the bond lengths in adduct **6a** are significantly longer, indicating relatively weak bonds consistent with the observed dissociation in presence of other donor molecules like THF. The distance between cationic and anionic tin atoms (4.5258(3) Å) is larger than the sum of vdW radii (4.32 Å)[21] excluding direct interaction. By contrast, the distance between the cationic tin atom Sn1 and anionic bromine atom Br2 (3.3254(4) Å) is below the sum of the vdW radii (4.03 Å),[21] whereas the distances between cationic Sn1 and Br3 (5.6577(5) Å) or Br4 (6.7314(4) Å) are significantly larger, indicating no interaction. The Br1-Sn1 bond (2.6155(4) Å) in the cation of **6a** is slightly longer than the Sn–Br bond in $SnBr_2$ bromide (2.55 Å),[22] similar to the Sn–Br bond lengths in the $[SnBr_3]^-$ anion (2.6123(4) Å and 2.6941(4) Å).

Mass spectrometric techniques such as Electrospray Ionisation (ESI) and Laser Desorption Ionization without an assistant matrix (LDI) led to fragmentation during the ionization process. Further, the identity and purity of neat product **6a** is confirmed by elemental analysis.

To increase the solubility and to avoid dynamic exchange, **6a** was reacted with $Li[Al(OC(CF_3)_3)_4]$ in dichloromethane solution (Scheme 4). As intended **6b** shows an increased solubility compared with **6a** and can be separated easily from the precipitated by-product $LiSnBr_3$. The ^{31}P-NMR spectra of **6b** show singlet resonances at 3.3 ppm (95 %, *cis* isomer) and 6.5 ppm (5 %, *trans* isomer) with reduced line broadening (**6b** (^{31}P) $\nu_{1/2}$ = 100 Hz, compared to **6a** (^{31}P) $\nu_{1/2}$ = 170 Hz). The anion exchange causes a downfield shift of ca. 8 ppm for the *cis* isomer, while the chemical shift of the *trans* isomer remains nearly unchanged. Interestingly, for the ^{31}P-NMR signal of *cis*-**6b** the J_{PSn} coupling can be observed as satellites ($^1J_{PSn}$ = 1400 Hz (^{119}Sn isotopomer), $^1J_{PSn}$ = 1240 Hz (^{117}Sn isotopomer)), which is not possible for *trans*-**6b** owing to the weak signal intensity. The observed J_{PSn} coupling constants are consistent with literature data.[3b,23] Despite observing tin satellites in the ^{31}P-NMR spectra of **6b**, no ^{119}Sn-NMR signals of **6b** could be observed. In the ^{1}H-NMR-spectra of **6b**, the PH protons are slightly deshielded relative to **6a** with the *cis* isomer resonating at 6.03 ppm (d, $^1J_{PH}$ = 360.0 Hz) while the signal of the *trans* isomer is found at 5.78 ppm (d, $^1J_{PH}$ = 364.3 Hz). The ^{27}Al-NMR spectrum of **6b** shows a narrow singlet at 34.7 ppm ($\nu_{1/2}$ = 13 Hz) characteristic for the aluminate species in this weakly coordinating anion.[24] Furthermore, the identity and purity of **6b** was confirmed by elemental analysis.

Moving to the next heavier tetrel, we explored the reaction of **5** with equimolar amounts of $PbCl_2$ and $AlCl_3$ in dichloromethane. (Scheme 5). Within a few hours all solids dissolved resulting in an orange-red, clear solution. The ^{31}P-NMR spectra of the solution show a very broad signal ranging from 59 ppm to 50 ppm ($\nu_{1/2}$ = 1000 Hz) with no resolved ^{207}Pb-satellites. Significant broadening is observed in the ^{1}H-NMR spectra where the PH resonances at 6.10 ppm ($^1J_{PH}$ = 332 Hz) and 5.73 ppm ($^1J_{PH}$ = 336 Hz) are deshielded relative to the starting material. The ^{1}H and ^{13}C-NMR spectra are consistent with the formation of μ-bridged dimeric adduct **7**. The ^{1}H-NMR spectrum shows seven multiplets in the range of 5.02 to 4.45 ppm for the Cp hydrogen atoms, while the protons of *tert*-butyl groups are found as a multiplet (1.37–1.28 ppm). The corresponding ^{13}C-NMR spectrum of **7** reveals eight multiplets, while some of the for α- and β-Cp carbon atoms are observed as pseudo triplets in the range of 79.3 ppm to 72.8 ppm. Those pseudo triplets are characteristic for a successful ring formation and are observed for many diphospha [3]ferrocenophanes.[3a,b,16]

The tetrachloroaluminate counter anion in **7** features a singlet resonance at 103.9 ppm ($\nu_{1/2}$ = 250 Hz) in the ^{27}Al-NMR spectra, for which the relatively narrow line width can be attributed to the high symmetry of the anion.[11] By contrast, no ^{207}Pb-NMR resonance could be detected which may be a consequence of extreme broadening owing to fast relaxation.[11,19, 25]

Our attempts to characterize **7** using Electrospray Ionisation (ESI) remained unsuccessful as well, since the compound decomposed during the ionization process. Nevertheless, identity and purity of **7** were further corroborated by elemental analysis.

Owing to its low solubility, bisphosphonio plumbylene **7** crystallizes readily from the reaction mixture in the monoclinic space group *C*2/*c*. The asymmetric unit contains half of the molecule, whereas the molecular structure depicted in Figure 5 is generated by symmetry operations.

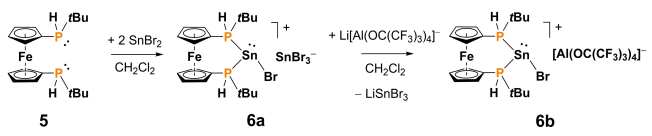

Scheme 4. Coordination of Sn(II) with **5** followed by anion exchange.

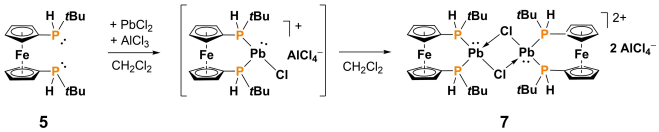

Scheme 5. Coordination of Pb(II) with **5** in presence of an additional Lewis acid.

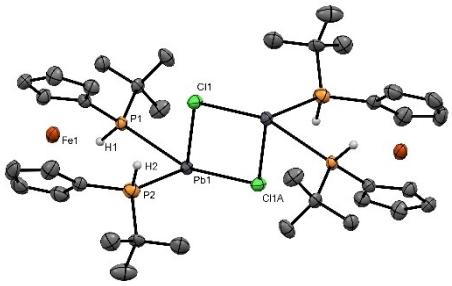

Figure 5. Molecular structure of **7**. Ellipsoids are drawn at 30% probability level. The hydrogen atoms, except those attached to the phosphorus atoms and the tetrachloroaluminate anions are omitted for clarity. Selected bond lengths and angles: P1-Pb1 2.935(2) Å; Pb1-Cl1 2.620(2) Å; P2-Pb1 2.915(3) Å; Pb1-Cl1 A 3.035(2) Å; P1-H1 1.33(13) Å P2-H2 1.29(10) Å; P1-Pb1-P2 87.50(7)°.

In contrast to its stannylene analog **6a**, plumbylene **7** stabilizes by intermolecular dimerization via μ-Cl bridges, similar to other lead chlorides.[19,26] Symmetric contacts are found between Pb1 and both phosphorus atoms with bond lengths of Pb1-P1 2.935(2) Å and Pb1-P2 2.915(3) Å. Literature known low coordinate lead(II) complexes show Pb–P bond lengths between 2.715(5) Å and 2.971(5) Å.[3d,27] The Pb_2Cl_2 unit forms a diamond-shaped planar ring with an intramolecular Pb1-Cl1 distance of 2.620(2) Å which is significantly shorter compared to the intermolecular Pb1-Cl1A distance of 3.035(2) Å, by 0.415 Å. Comparable Pb–Cl bond lengths have been reported for intermolecularly stabilized μ-chlorobridged bisplumbylene with 2.6440(1) Å (intramolecular) and 3.2677(2) Å (intermolecular), showing a larger Pb–Cl distance difference of Δ(Pb–Cl) = 0.628 Å.[19,27a] The Pb–Pb distance (4.4450(7) Å) is larger than the sum of the vdW radii (4.04 Å)[21] not supporting direct interaction. The distance between the cationic lead atom Pb1 and anionic chloride atom Cl2 (3.264(3) Å) is also below the sum of the vdW radii (4.04 Å),[21] whereas the distances of cationic Pb1 to all other anionic chloride atoms (5.563(3) Å (Pb1-Cl4)–6.521(2) Å (Pb1-Cl3)) are significantly larger, indicating no interaction. The interpretation of the bonding situation of **7** was verified by DFT calculations at the ωB97X-D/def2-SVP level of theory. The Wiberg bond index of the Pb1-Cl1 bond is 0.91, while 0.29 was computed in case of the intermolecular Pb1-Cl1 A bond. Results of Bader's analysis are in agreement with the Wiberg bond index, the electron densities are 0.052 au (Pb1-Cl) and 0.019 au (Pb1-Cl1A) in the bond critical points. No bond critical point was found between the lead atoms, therefore a direct Pb–Pb interaction can be excluded.

Remarkably, compound **7** is the dimer of the *rac* diastereomer in contrast to most other diphospha[3]ferrocenophanes occurring in the *meso* form.[3a,18] Accordingly, the PH hydrogen atoms in **7** are arranged in *trans* orientation with PH bond lengths (P1-H1: 1.20(12) Å, P2-H2: 1.16(8) Å) being slightly shorter compared to those in **6a** (P1-H1: 1.33(13) Å, P2-H2: 1.29(10) Å). The P–Pb-P angle in **7** is 87.50(7)° which is significantly larger than the P–Sn-P (77.79(3)°) angle in adduct **6a**, or structurally related compounds where P–Pb-P angles range between 68° and 79°.[3d,19] The Cp rings in **7** are found in a staggered conformation ($\tau = 50°$) and are arranged nearly coplanar ($\alpha = 0.3(4)°$), indicating no ring strain in the ferrocenophane bridge. Preliminary investigations exploring the electrochemical properties even for ligand **5** alone indicate irreversible to quasi-reversible behavior depending on the potential scan rate (cf. figures S15-17 in the ESI for details). These findings would be consistent with an initial iron centered oxidation followed by intramolecular SET from P^{III} to Fe^{III} in analogy to a closely related example studied in depth, previously.[16]

Conclusions

We have shown that 1,1′-ferrocenylenen bisphosphanes are well suited for the donor stabilization of Sn(II) and Pb(II) fragments depending on the substitution pattern at the phosphanyl units. The donor stabilization exerted by commercially available dppf is limited and cyclic bisphosphoniostannylenes are only accessible with additional Lewis acids which likewise compete with the donor precluding formation of the corresponding bisphosphonioplumbylenes. By contrast, with bisphosphane **5** the cyclic bisphosphoniostannylene is formed even in the absence of additional Lewis acids and the related bisphosphonioplumbylene can be obtained as well, albeit in dimeric form. Generally, the situation is complicated by dynamic exchange in solution requiring a comparative approach in solution and solid phase based on XRD and solid state NMR spectroscopy. The dynamic nature can be effectively suppressed by employing anion exchange with weakly coordinating anions. Based on this general entry, we will further vary the nature of the underlying bisphosphanes in the future to explore displacement of the halide donor and interaction with potential substrates.

Supporting Information

The authors have cited additional references within the Supporting Information (Ref [27–33]).

Acknowledgements

R.P. thanks the German Science Fund (DFG) for financial support (CRC 1319 ELCH). T.G. thanks the CRC 1487 Iron Upgraded for financial support. We thank Prof. Buntkowsky (TU Darmstadt) for generous allocation of measurement time at his Bruker Avance III 600 MHz spectrometer. Z. K. is grateful for the general support of János Bolyai Research Scholarship and Project UNKP-23-5 BME-419. Open Access funding enabled and organized by Projekt DEAL.

Conflict of Interests

The authors declare no conflict of interest.

Data Availability Statement

The data that support the findings of this study are available in the supplementary material of this article.

Keywords: tin · lead · phosphorus · ferrocene · tetrylene

[1] a) R. C. Fischer and P. P. Power, *Chem. Rev.* **2010**, *110*, 3877–3923; b) P. P. Power, *Chem. Rev.* **1999**, *99*, 3463–3503.
[2] M. Kira, T. Iwamoto, S. Ishida, *Bull. Chem. Soc. Jpn.* **2007**, *80*, 258–275.
[3] a) D. Kargin, Z. Kelemen, K. Krekić, M. Maurer, C. Bruhn, L. Nyulászi, R. Pietschnig, *Dalton Trans.* **2016**, *45*, 2180–2189; b) D. Kargin, Z. Kelemen, K. Krekić, L. Nyulászi, R. Pietschnig, *Chem. Eur. J.* **2018**, *24*, 16774–16778; c) K. Izod, J. Stewart, E. R. Clark, W. Clegg, R. W. Harrington, *Inorg. Chem.* **2010**, *49*, 4698–4707; d) A. H. Cowley, D. M. Giolando, R. A. Jones, C. M. Nunn, J. M. Power, *Polyhedron* **1988**, *7*, 1909–1910; e) W.-W. du Mont, H.-J. Kroth, *Angew. Chem. Int. Ed.* **1977**, *16*, 792–793.
[4] K. Izod, P. Evans, P. G. Waddell, *Angew. Chem. Int. Ed.* **2017**, *56*, 5593–5597.
[5] a) K. Izod, D. G. Rayner, S. M. El-Hamruni, R. W. Harrington, U. Baisch, *Angew. Chem. Int. Ed.* **2014**, *53*, 3636; b) M. Driess, R. Janoschek, H. Pritzkow, S. Rell, U. Winkler, *Angew. Chem. Int. Ed.* **1995**, *34*, 1614–1616.
[6] a) L. Nyulaszi, *Tetrahedron* **2000**, *56*, 79–84; b) J. Kapp, C. Schade, A. M. El-Nahasa, P. von Ragué Schleyer, *Angew. Chem. Int. Ed.* **1996**, *35*, 2236–2238.
[7] C. Gurnani, A. L. Hector, E. Jager, W. Levason, D. Pugh, G. Reid, *Dalton Trans.* **2013**, *42*, 8364–8374.
[8] S. Biswas, N. Patel, R. Deb, M. Majumdar, *Chem. Rec.* **2022**, *22*, e202200003.
[9] S. A. Weicker, J. W. Dube, P. J. Ragogna, *Organometallics* **2013**, *32*, 6681–6689.
[10] R. K. Raut, P. Sahoo, D. Chimnapure, M. Majumdar, *Dalton Trans.* **2019**, *48*, 10953–10961.
[11] R. K. Harris, *NMR and the periodic table*, Acad. Press, London, **1978**, p.
[12] J.-P. Laussac, *Org. Magn. Reson.* **1979**, *12*, 237–242.
[13] J. Burt, W. Levason, M. E. Light and G. Reid, *Dalton Trans.* **2014**, *43*, 14600–14611.
[14] R. L. Wells, A. T. McPhail, J. A. Laske and P. S. White, *Polyhedron* **1994**, *13*, 2737–2744.
[15] a) S. Dey and R. Pietschnig, *Coord. Chem. Rev.* **2021**, *437*, 213850; b) S. Dey, D. Buzsáki, C. Bruhn, Z. Kelemen and R. Pietschnig, *Dalton Trans.* **2020**, *49*, 6668–6681.
[16] A. Lik, D. Kargin, S. Isenberg, Z. Kelemen, R. Pietschnig, H. Helten, *Chem. Commun.* **2018**, *54*, 2471–2474.
[17] J.-C. Hierso, A. Fihri, R. Amardeil, P. Meunier, H. Doucet, M. Santelli, B. Donnadieu, *Organometallics* **2003**, *22*, 4490–4499.
[18] S. Borucki, Z. Kelemen, M. Maurer, C. Bruhn, L. Nyulászi, R. Pietschnig, *Chem. Eur. J.* **2017**, *23*, 10438–10450.
[19] D. Kargin in *Donor-stabilisierte Bisphosphanyl-Tetrylene*, *Vol. Ph.D.* University of Kassel, **2019**, 71.
[20] S. Hitzel, C. Färber, C. Bruhn, U. Siemeling, *Dalton Trans.* **2017**, *46*, 6333–6348.
[21] A. Bondi, *J. Phys. Chem.* **1964**, *68*, 441–451.
[22] J. L. Wardell, *Tin: Inorganic Chemistry*, Wiley, Chichester, New York, **1994**.
[23] S. Berger, S. Braun, H.-O. Kalinowski, *^{31} P-NMR-Spektroskopie*, Georg Thieme Verlag, Stuttgart, Germany, **1993**.
[24] I. Krossing, *Chem. Eur. J.* **2001**, *7*, 490–502.
[25] L. Pu, B. Twamley, P. P. Power, *Organometallics* **2000**, *19*, 2874–2881.
[26] D. Kargin, K. Krekić, R. Pietschnig, *Eur. J. Inorg. Chem.* **2019**, 1650–1656.
[27] a) D. Kargin, K. Krekić, R. Pietschnig, *Z. Anorg. Allg. Chem.* **2018**, *644*, 1051–1056; b) A. L. Balch, D. E. Oram, *Inorg. Chem.* **1987**, *26*, 1906–1912.
[28] a) I. Scholz, P. Hodgkinson, B. H. Meier, M. Ernst, *J. Chem. Phys.* **2009**, *130*, 114510; b) A. E. Bennett, C. M. Rienstra, M. Auger, K. V. Lakshmi, R. G. Griffin, *J. Chem. Phys.* **1995**, *103*, 6951–6958.
[29] D. Massiot, F. Fayon, M. Capron, I. King, S. Le Calvé, B. Alonso, J. O. Durand, B. Bujoli, Z. Gan, G. Hoatson, *Magn. Reson. Chem.* **2002**, *40*, 70–76.
[30] G. Sheldrick, *Acta Crystallogr. Sect. C* **2015**, *71*, 3–8.
[31] O. V. Dolomanov, L. J. Bourhis, R. J. Gildea, J. A. K. Howard, H. Puschmann, *J. Appl. Crystallogr.* **2009**, *42*, 339–341.
[32] C. F. Macrae, P. R. Edgington, P. McCabe, E. Pidcock, G. P. Shields, R. Taylor, M. Towler, J. van de Streek, *J. Appl. Crystallogr.* **2006**, *39*, 453–457.
[33] M. J. Frisch, G. W. Trucks, H. B. Schlegel, G. E. Scuseria, M. A. Robb, J. R. Cheeseman, G. Scalmani, V. Barone, G. A. Petersson, H. Nakatsuji, X. Li, M. Caricato, A. V. Marenich, J. Bloino, B. G. Janesko, R. Gomperts, B. Mennucci, H. P. Hratchian, J. V. Ortiz, A. F. Izmaylov, J. L. Sonnenberg, D. Williams-Young, F. Ding, F. Lipparini, F. Egidi, J. Goings, B. Peng, A. Petrone, T. Henderson, D. Ranasinghe, V. G. Zakrzewski, J. Gao, N. Rega, G. Zheng, W. Liang, M. Hada, M. Ehara, K. Toyota, R. Fukuda, J. Hasegawa, M. Ishida, T. Nakajima, Y. Honda, O. Kitao, H. Nakai, T. Vreven, K. Throssell, J. A. Montgomery Jr., J. E. Peralta, F. Ogliaro, M. Bearpark, J. J. Heyd, E. Brothers, K. N. Kudin, V. N. Staroverov, T. Keith, R. Kobayashi, J. Normand, K. Raghavachari, A. Rendell, J. C. Burant, S. S. Iyengar, J. Tomasi, M. Cossi, J. M. Millam, M. Klene, C. Adamo, R. Cammi, J. W. Ochterski, R. L. Martin, K. Morokuma, O. Farkas, J. B. Foresman, D. J. Fox, *Gaussian 16, Revision C.01*, Gaussian, Inc., Wallingford CT, **2016**.
[34] T. Lu, F. Chen, *J. Comput. Chem.* **2012**, *33*, 580–592.

Manuscript received: October 30, 2023
Revised manuscript received: December 13, 2023
Accepted manuscript online: December 13, 2023
Version of record online: December 27, 2023